

# Spontaneous Parity Breaking in Quantum Antiferromagnets on the Triangular Lattice

Songtai Lv,<sup>1</sup> Yuchen Meng,<sup>1</sup> and Haiyuan Zou<sup>1,\*</sup>

<sup>1</sup>*Key Laboratory of Polar Materials and Devices (MOE),  
School of Physics, East China Normal University, Shanghai 200241, China*

Frustration on the triangular lattice has long been a source of intriguing and often debated phases in many-body systems. Although symmetry analysis has been employed, the role of the seemingly trivial parity symmetry has received little attention. In this work, we show that phases induced by frustration are systematically shaped by an implicit rule of thumb associated with spontaneous parity breaking. This principle enables us to anticipate and rationalize the regimes and conditions under which nontrivial phases emerge. For the spin- $S$  antiferromagnetic XXZ model, we demonstrate that a controversial parity-broken phase appears only at intermediate values of  $S$ . In bilayer systems, enhanced frustration leads to additional phases, such as supersolids, whose properties can be classified by their characteristic parity features. Benefiting from our improved tensor network contraction techniques, we confirm these results through large-scale tensor-network calculations. This study offers an alternative viewpoint and a systematic approach for examining the interplay between spin, symmetry, and frustration in many-body systems.

*Introduction.* Geometrically frustrated systems, with the triangular lattice as a paradigmatic example, host a wide variety of exotic phases and emergent phenomena [1–6], including but not limited to supersolids, quantum spin liquids, and unconventional critical behaviors [7–16]. When an external magnetic field is applied, additional richness arises in the form of magnetization plateaus [17–21], analogous to Hall plateaus in electronic systems. Remarkably, even in the absence of explicitly introduced symmetry-breaking terms such as Dzyaloshinskii–Moriya interactions, quantum fluctuations alone can stabilize numerous phases in the vicinity of these magnetization plateaus [22–25]. Some of these phases remain under debate; however, such controversies are themselves informative, as they motivate the search for deeper organizing principles underlying phase competition in frustrated systems.

In recent years, experimental progress on triangular-lattice magnets has advanced rapidly, while a number of exotic phases continue to defy clear understanding [5, 26]. Various theoretical and numerical approaches, including cluster methods [27, 28], density-matrix renormalization group (DMRG) [22, 24, 29], and tensor-network methods [30–32], have been employed to investigate these phase competitions; however, the very richness of phases in triangular-lattice systems inevitably leads to pronounced method dependence: different numerical approaches may yield conflicting conclusions regarding the existence or stability region of a given phase, even for states with well-established ordering patterns, let alone quantum spin liquids. This situation underscores the need for more powerful and reliable numerical methods, which must incorporate physically motivated entanglement structures and respect fundamental theoretical constraints intrinsic to frustrated systems.

For this reason, the symmetries of the system are usually taken into account [3]; however, parity, which is crucial in the study of topology [33], has rarely been employed as a guiding principle for analyzing its im-

pact on frustrated quantum many-body systems. As two counterintuitive examples in antiferromagnetic (AF) spin models on the triangular lattice, consider the V-shaped phase (Fig. 2), which appears mirror-asymmetric, in fact possesses an overlooked parity symmetry. In contrast, the mirror-symmetric Fan phase (Fig. 2) actually breaks parity. This observation naturally raises a fundamental question: are there universal parity-breaking principles that can account for the existence and stability of these phases? Moreover, the emergence of phases with classical analog configurations is typically driven by quantum order-by-disorder effects, whose strength depends on the spin magnitude  $S$ . Numerical results such as tensor networks at larger  $S$  are therefore crucial. However, the rapidly increasing computational complexity has so far limited systematic comparisons between numerical results and theoretical expectations.

Motivated by these considerations, as well as by the celebrated Lee–Yang’s result on parity violation in weak interactions [34], we propose a rule-of-thumb parity principle that applies to the AF triangular-lattice XXZ (TLXXZ) model for arbitrary  $S$ : in frustration-induced spin-ordered phases, parity is spontaneously broken, while increasing a longitudinal magnetic field tends to restore parity symmetry. As a corollary, paramagnetic phases (e.g., valence-bond-solid states) stabilized by additional frustration (e.g., in bilayer systems) are expected to preserve parity, whereas tuning the external field which compete with frustration may lead to sequences in which parity is first broken and subsequently restored.

To substantiate these ideas, we have developed an improved and accelerated corner-transfer-matrix renormalization group (CTMRG) contraction scheme, enabling large-scale tensor-network simulations for different  $S$  as well as bilayer geometries. Our results confirm the proposed parity principle, clarify the long-debated existence and parameter regime of the Fan phase at large  $S$ , and characterize the parity properties of supersolid phases in

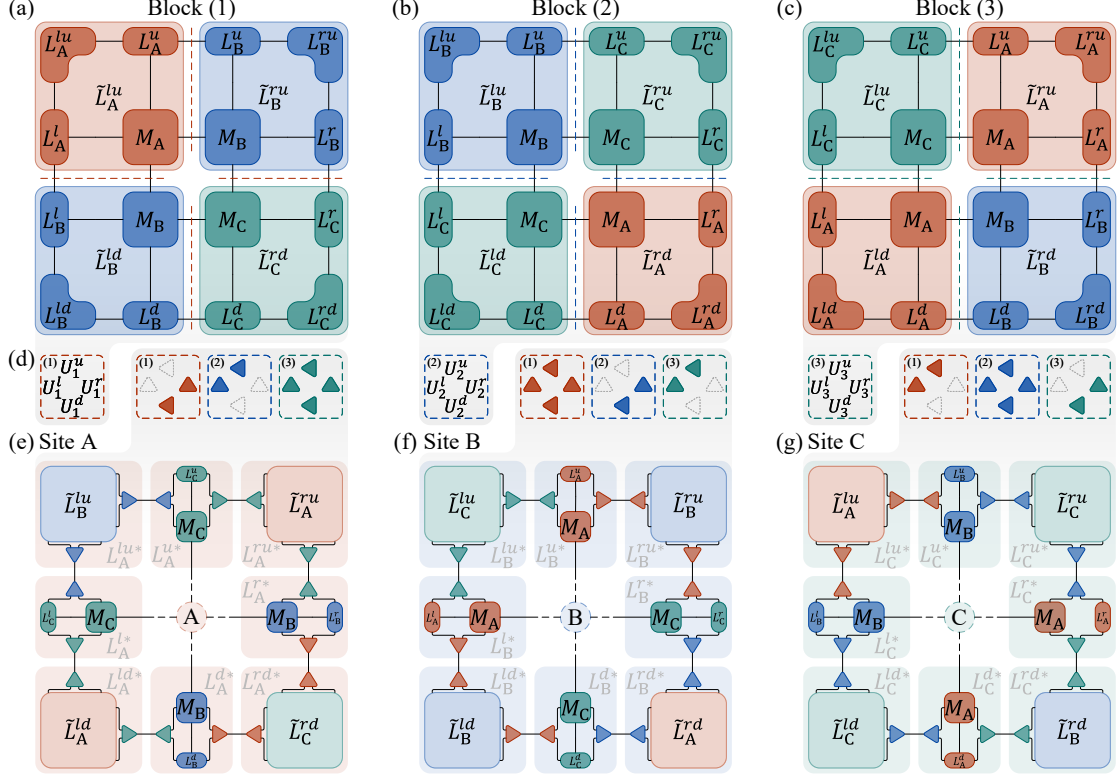


FIG. 1. CTMRG procedure for the triangular lattice. (a–c) Three blocks arising from the triangular-lattice periodicity, each composed of local tensors  $M_i$  ( $i = A, B, C$ ) together with their associated edge tensors  $L_i^\mu$  ( $\mu = l, d, r, u$ ) and corner tensors  $L_i^{\mu\nu}$  ( $\mu\nu = lu, ld, rd, ru$ ). (d) Isometries  $U_n^\mu$  ( $n = 1, 2, 3$ ) obtained from singular-value decompositions at the dashed cuts in (a–c) are shown. Solid triangles indicate the position of  $U_n^\mu$  for the next step. (e–g) Update of the environment tensors through contractions with  $U_n^\mu$  and  $U_n^{\mu\dagger}$ , yielding the renormalized  $L_i^{\mu*}$  and  $L_i^{\mu\nu*}$ .

bilayer systems. By resolving several long-standing and controversial theoretical issues, our findings also provide valuable insight for interpreting experimental observations in triangular-lattice magnets.

*TLXXZ model.* We first consider the two-dimensional TLXXZ model, described by the Hamiltonian,

$$H = J_{ab} \sum_{\langle i,j \rangle_{ab}} (S_i^x S_j^x + S_i^y S_j^y + \eta S_i^z S_j^z) - h_z \sum_i S_i^z, \quad (1)$$

where  $J_{ab}$  denotes the nearest-neighbor exchange interaction. The operator  $S_i$  represents the spin at site  $i$ , the anisotropy parameter  $\eta \leq 1$  is considered, and  $h_z$  is the longitudinal magnetic field. For  $S = 1/2$ , the phase diagram in the plane of  $h_z$  and  $\eta$  is widely studied [23, 24]. It includes phases such as the umbrella phase, the up-up-down (uud) phase, the Y phase, and the V phase. The existence and location of the Fan phase, however, remain controversial: cluster-based approaches place it between the ferromagnetic (FM), V, and umbrella phases [23], whereas DMRG calculations have not found evidence for its stability [24].

We also consider the bilayer TLXXZ model, for which

the Hamiltonian contains an additional interlayer term

$$H' = J_c \sum_{\langle i,j \rangle_c} \vec{S}_i \cdot \vec{S}_j + J_d \sum_{\langle\langle i,j \rangle\rangle} \vec{S}_i \cdot \vec{S}_j, \quad (2)$$

where  $J_c$  denotes the coupling along the  $c$ -axis between the interlayer pairs ( $\langle i, j \rangle_c$ ). The coupling  $J_d$  represents the interlayer next-nearest-neighbor interaction between pairs  $\langle\langle i, j \rangle\rangle$ . In the absence of a magnetic field, sufficiently large  $J_c$  drives the bilayer system into a dimerized phase with interlayer spin singlets. Upon increasing the longitudinal field, the system successively exhibits the 1/3 and 2/3 magnetization plateaus before saturation, as well as additional supersolid phases and Bose–Einstein–condensed (BEC) phases [35].

*CTMRG procedure for the TLXXZ model.* Following Ref. [32], we construct a projected entangled simplex state (PESS) ansatz [31] using a unit cell consisting of three local tensors and three simplex tensors, and evolve the state until convergence. By contracting each local tensor with the associated simplex tensors and tracing over the physical indices, we obtain three rank-four tensors  $M_i$ , ( $i = A, B, C$ ), which serve as the building blocks for two-dimensional coarse graining. This contraction is carried out using the CTMRG method. Originating

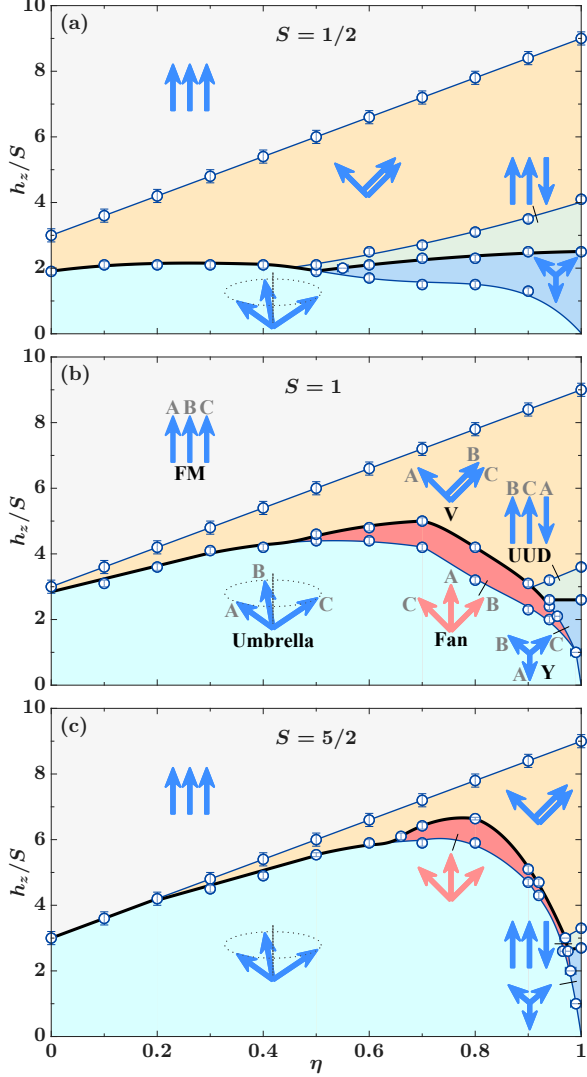


FIG. 2. Ground state phase diagrams of the monolayer TLXXZ model for  $S = 1/2, 1$ , and  $5/2$ , shown in panels (a-c), respectively. Circles with error bars are the calculated boundaries, while solid curves are guides to the eye. Thick black lines denote parity-breaking phase transitions. Arrows represent spin configurations (FM, Umbrella, V, Y, and UUD) on the  $A$ ,  $B$ , and  $C$  sublattices.

from a DMRG algorithm [36], CTMRG has undergone substantial developments alongside tensor-network techniques [37–42] and has become a key tool for tensor-network simulations in the thermodynamic limit.

Here, we propose a more highly parallelized CTMRG scheme that significantly improves computational efficiency. The main difference from conventional CTMRG lies in the fact that our approach avoids performing multiple directional cuts to construct the dimension-reducing isometry  $U$ , and does not require repeatedly contracting singular values back into the target tensor along four separate directions. Instead, our method simultaneously

generates all  $U$ s required for evolution along the four lattice directions, enabling the entire coarse-graining step to be completed in a single operation. This procedure can be straightforwardly generalized to unit cells containing a larger number of inequivalent tensors.

Specifically, taking the case of three tensors as an example (Fig. 1), the environment of each tensor ( $M_i$ ) is constructed from four edge tensors and four corner tensors. By considering configurations composed of four  $M_i$  tensors, all three possible connectivity patterns are included. For each configuration, matrices are formed by cutting the network along the four lattice directions (indicated by dashed lines), thereby encoding the full environmental information of  $M_i$  in the up, down, left, and right directions. Singular value decomposition (SVD) of these matrices yield twelve isometries  $U_i$ , which are then simultaneously inserted on both sides of all environment tensors according to the lattice geometry, realizing a one-step evolution of the entire environment. After convergence, physical observables such as the ground-state energy, local magnetization, and correlation functions can be readily evaluated. Using a virtual bond dimension ( $D_b = 4$ ) for the local tensors (with CTMRG truncation dimension ( $\chi = 48$ ), we obtain a ground-state energy of  $E_0 = -0.1824$  for the triangular-lattice AF Heisenberg model at zero field, in agreement with results obtained from other CTMRG-based approaches [32].

*Phase diagrams of the monolayer TLXXZ model.* Using the above-developed method, we perform large-scale simulations of the TLXXZ model for  $S = 1/2, 1$ , and  $5/2$ , and obtain comprehensive ground-state phase diagrams in the  $\eta$ - $h$  plane (Fig. 2). For the  $S = 1/2$  case, aside from some minor differences in details, our results for the coplanar V, UUD, and Y phases, as well as the noncoplanar umbrella phase, are in agreement with previous studies. [23, 24]. Notably, we do not find any evidence for the Fan phase, in agreement with DMRG results [24]. This absence can be naturally understood within the parity-symmetry analysis discussed above. Choosing site  $A$  as the parity center, the  $B$  and  $C$  sublattices are exchanged under a parity transformation, while spins, being pseudovectors, remain invariant. Consequently, the zero-field  $120^\circ$  phase, the umbrella, UUD, and Y phases at small fields all exhibit spontaneous parity breaking. In contrast, the high-field FM and V phases preserve parity symmetry. The latter may appear counterintuitive at first sight, since the apparent asymmetry in commonly used arrow representations of spins can obscure the underlying parity invariance of the V phase.

At zero field, frustration stabilizes the  $120^\circ$  ground state and breaks parity symmetry. The applied field  $h_z$  introduces FM alignment, which is the only mechanism counteracting the intrinsic AF correlations in the ( $S^z$ ) component. As  $h_z$  increases, parity-broken phases (Y and umbrella) give way to parity-preserving phases (UUD and V). Further increasing  $h_z$  continues to protect parity symmetry, making it difficult for a parity-breaking

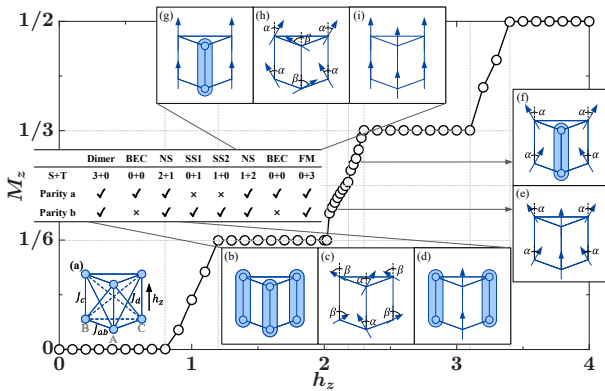


FIG. 3. Magnetization  $M_z$  of the bilayer TLXXZ model with varied  $h_z$ . Inset (a) illustrates the lattice geometry and couplings, and insets (b–i) show representative spin configurations of each phase. The table lists the numbers of singlets (S) and triplets (T), as well as whether parity a and parity b are preserved.

Fan phase to emerge between the FM and V phases. In fact, the Fan phase can appear only if the suppression of classically ordered states by quantum order-by-disorder effects is reduced. In other words, it can be stabilized only by increasing  $S$ , while the parity rule of thumb remains valid. E.g., in the classical limit  $S \rightarrow \infty$ , only a direct transition from the umbrella phase to the FM phase occurs, implying that the Fan phase, if present, must appear before the parity-preserving V phase as  $h_z$  is increased.

Our results for larger spins,  $S = 1$  and  $5/2$ , are fully consistent with this picture. With increasing  $S$ , the umbrella phase shifts to higher fields and eventually connects directly to the FM phase in the classical limit. Along this evolution, the Fan phase emerges and occupies the region between the umbrella and V phases, leading to a parity-restoring transition from the Fan to the V phase. In addition, near  $\eta = 1$ , the UUD and Y phases become strongly compressed in the large  $\eta$  range as  $S$  increases, consistent with experimental observations of much weaker  $1/3$  magnetization plateaus in spin- $5/2$  systems [43, 44].

*Dimer breaking in the bilayer TLXXZ model.* Our approach can be straightforwardly extended to bilayer systems, where additional couplings give rise to competition among a much richer set of exotic phases. Here we focus on the  $S = 1/2$  isotropic case ( $\eta = 1$ ) and choose a parameter regime with dominant interlayer coupling ( $J_{ab} = 0.425$ ,  $J_c = 1$ ,  $J_d = 0.325$ ) to stabilize interlayer dimerization. As  $h_z$  is increased, we explicitly confirm the emergence of the  $1/3$  and  $2/3$  magnetization plateaus [35], corresponding respectively to configurations with two remaining singlets and with one remaining singlet per unit cell during the progressive destruction of dimers (Fig. 3). We identify all spin configurations along this process, and

find that the spins are coplanar in all these phases. Between the plateaus and the fully dimerized or fully polarized limits, the system enters BEC phases in which each individual layer realizes a V-type configuration. Between the two plateaus, two supersolid phases appear and exhibit Fan-like structure in each layer.

We interpret this evolution again from the perspective of spontaneous parity breaking. Unlike the single-layer case, where the  $h_z$  competes mainly with intralayer antiferromagnetism, here the field must additionally compete with multiple interlayer couplings. First, at  $h_z = 0$ , the strong AF interlayer coupling ( $J_c$ ) favors dimer formation and thereby restores parity symmetry. When  $J_{ab} = J_d$ , the competition between these two couplings effectively cancels interactions among the three dimers, such that increasing  $h_z$  drives the system directly from the fully dimerized state through the  $1/3$  and  $2/3$  plateaus to the fully polarized state. In this case, dimers are replaced by triplets one by one without breaking parity. The BEC and supersolid phases appear only when  $J_{ab} \neq J_d$ , where directional correlations among dimers become energetically favored and intermediate phases are stabilized between the plateaus.

In a bilayer structure, two distinct parities can be considered. The first, denoted parity a, treats each interlayer dimer as an effective unit and is thus analogous to the parity symmetry of the single-layer system. The second, parity b, resolves the bilayer structure explicitly, with the parity center chosen at the midpoint between the two layers at site A. For parity a, the transitions from the three-dimer state to the  $1/3$  plateau, and from the  $2/3$  plateau to FM phase, involve only modifications of the configuration at site A; the exchange of B and C sublattices under parity remains unaffected. Therefore, the intermediate BEC phases preserve parity a. In contrast, the supersolid phases necessarily involve choosing either the B or C sublattice on which a dimer is removed, thereby breaking parity a. This sequence can also be understood as a consequence of the competition between the field-induced ferromagnetism and the additional interlayer AF couplings. When  $h_z$  becomes comparable to  $J_d$ , it effectively compensates the interlayer interaction, rendering the system analogous to the single-layer case in which parity breaking can occur. Further increasing  $h_z$  then drives the system along the same trend as in the single-layer model, eventually restoring parity symmetry in the fully polarized state. For parity b, which resolves the detailed bilayer structure, the situation depends more sensitively on the competition between  $J_{ab}$  and  $J_d$ . During the transition from the three-dimer state to the  $1/3$  plateau, the BEC phase involves the breaking of dimers on the B and C sites as well, and is accompanied by the breaking of parity b. By contrast, in the two supersolid phases, we find that parity b is remarkably preserved. This reveals a more subtle and distinctive internal parity structure of supersolid phases in bilayer systems, which is absent in their single-layer counterparts.

*Summary and outlook.* In this work, by systematically investigating the AF TLXXZ model for  $S = 1/2$ , 1, and 5/2 using an improved CTMRG scheme, we uncover a previously overlooked rule of thumb governing parity breaking, as well as the impact of frustration on parity. With increasing external longitudinal field, parity generally exhibits a tendency toward symmetry restoration. The long-debated Fan phase is found to emerge only for  $S \geq 1$ . In bilayer systems, the presence of additional frustration leads to phases such as supersolids with much richer parity structures. Our results have direct implications for a broad class of triangular-lattice experiments. For instance, in spin-5/2 materials, the extent of the 1/3 magnetization plateau varies significantly among different compounds, with some exhibiting extremely narrow plateau regions. This behavior is consistent with our phase diagrams, in which the UUD phase is strongly compressed. Building on our results, the inclusion of further frustration effects, such as next-nearest-neighbor interactions [14] and transverse fields [45, 46], may provide a natural explanation for additional exotic plateaus, including the 1/2 and 5/6 plateaus observed experimentally. More broadly, our analysis of the interplay between parity and frustration can be extended to other frustrated lattices. The modified CTMRG method presented here also offers a powerful and efficient tool for the study of quantum many-body physics.

*Acknowledgments*—We thank Jie Ma, Tian Shang, Deyan Sun, Zhiyuan Xie, Rong Yu, and Weiqiang Yu for helpful discussions. This work is supported by the National Natural Science Foundation of China (Grant No. 12274126).

---

\* hyzou@phy.ecnu.edu.cn

- [1] L. Balents, Spin liquids in frustrated magnets, *Nature* **464**, 199 (2010).
- [2] B. J. Powell and R. H. McKenzie, Quantum frustration in organic Mott insulators: from spin liquids to unconventional superconductors, *Rep. Prog. Phys.* **74**, 056501 (2011).
- [3] O. A. Starykh, Unusual ordered phases of highly frustrated magnets: a review, *Rep. Prog. Phys.* **78**, 052502 (2015).
- [4] B. Schmidt and P. Thalmeier, Frustrated two dimensional quantum magnets, *Phys. Rep.* **703**, 1 (2017).
- [5] D. S. Inosov, Quantum magnetism in minerals, *Adv. Phys.* **67**, 149 (2019).
- [6] J. Khatua, B. Sana, A. Zorko, M. Gomilšek, K. Sethupathi, M. S. R. Rao, M. Baenitz, B. Schmidt, and P. Khuntia, Experimental signatures of quantum and topological states in frustrated magnetism, *Phys. Rep.* **1041**, 1 (2023).
- [7] S. Wessel and M. Troyer, Supersolid hard-core bosons on the triangular lattice, *Phys. Rev. Lett.* **95**, 127205 (2005).
- [8] D. Heidarian and K. Damle, Persistent supersolid phase of hard-core bosons on the triangular lattice, *Phys. Rev. Lett.* **95**, 127206 (2005).
- [9] R. G. Melko, A. Parameshwari, A. A. Burkov, A. Vishwanath, D. N. Sheng, and L. Balents, Supersolid order from disorder: hard-core bosons on the triangular lattice, *Phys. Rev. Lett.* **95**, 127207 (2005).
- [10] M. Boninsegni and N. Prokof'ev, Supersolid phase of hard-core bosons on a triangular lattice, *Phys. Rev. Lett.* **95**, 237204 (2005).
- [11] Y. Shimizu, K. Miyagawa, K. Kanoda, M. Maesato, and G. Saito, Spin liquid state in an organic mott insulator with a triangular lattice, *Phys. Rev. Lett.* **91**, 107001 (2003).
- [12] C. Xu, F. Wang, Y. Qi, L. Balents, and M. P. Fisher, Spin liquid phases for spin-1 systems on the triangular lattice, *Phys. Rev. Lett.* **108**, 087204 (2012).
- [13] W. Liu, Z. Zhang, J. Ji, Y. Liu, J. Li, X. Wang, H. Lei, G. Chen, and Q. Zhang, Rare-earth chalcogenides: A large family of triangular lattice spin liquid candidates, *Chin. Phys. Lett.* **35**, 117501 (2018).
- [14] C. A. Gallegos, S. Jiang, S. R. White, and A. L. Chernyshev, Phase diagram of the easy-axis triangular-lattice  $J_1$ - $J_2$  model, *Phys. Rev. Lett.* **134**, 196702 (2025).
- [15] J. G. Rau, P. A. McClarty, and R. Moessner, Pseudo-Goldstone gaps and order-by-quantum disorder in frustrated magnets, *Phys. Rev. Lett.* **121**, 237201 (2018).
- [16] G. V. Chen, Emergent Berezinskii-Kosterlitz-Thouless and Kugel-Khomskii physics in the triangular lattice bilayer cobaltate, *Phys. Rev. Lett.* **133**, 136703 (2024).
- [17] S. Miyashita, Magnetic properties of Ising-like Heisenberg antiferromagnets on the triangular lattice, *J. Phys. Soc. Jpn.* **55**, 13 (1986).
- [18] A. V. Chubukov and D. I. Golosov, Quantum theory of an antiferromagnet on a triangular lattice in a magnetic field, *J. Phys.: Condens. Matter* **3**, 69 (1991).
- [19] H. Nojiri, Y. Tokunaga, and M. Motokawa, Magnetic phase transition of helical  $\text{CsCuCl}_3$  in high magnetic field, *Le Journal de Physique Colloques* **49**, C8 (1988).
- [20] T. Inami, Y. Ajiro, and T. Goto, Magnetization process of the triangular lattice antiferromagnets,  $\text{RbFe}(\text{MoO}_4)_2$  and  $\text{CsFe}(\text{SO}_4)_2$ , *J. Phys. Soc. Jpn.* **65**, 2374 (1996).
- [21] N. A. Fortune, S. T. Hannahs, Y. Yoshida, T. E. Sherline, T. Ono, H. Tanaka, and Y. Takano, Cascade of magnetic-field-induced quantum phase transitions in a spin- $\frac{1}{2}$  triangular-lattice antiferromagnet, *Phys. Rev. Lett.* **102**, 257201 (2009).
- [22] S.-i. Yoshikawa, K. Okunishi, M. Senda, and S. Miyashita, Quantum fluctuation-induced phase transition in  $S = 1/2$  XY-like Heisenberg antiferromagnets on the triangular lattice, *J. Phys. Soc. Jpn.* **73**, 1798 (2004).
- [23] D. Yamamoto, G. Marmorini, and I. Danshita, Quantum phase diagram of the triangular-lattice XXZ model in a magnetic field, *Phys. Rev. Lett.* **112**, 127203 (2014).
- [24] D. Sellmann, X.-F. Zhang, and S. Eggert, Phase diagram of the antiferromagnetic XXZ model on the triangular lattice, *Phys. Rev. B* **91**, 081104 (2015).
- [25] D. Yamamoto, T. Sakurai, R. Okubo, S. Okubo, H. Ohata, H. Tanaka, and Y. Uwatoko, Continuous control of classical-quantum crossover by external high pressure in the coupled chain compound  $\text{CsCuCl}_3$ , *Nat. Commun.* **12**, 4263 (2021).
- [26] M. Zhang, M. Shu, X. Shen, and J. Ma, Quantum effect of triple-perovskite antiferromagnets with triangular lattices,  $\text{A}_3\text{MB}_2\text{O}_9$  ( $\text{A} = \text{Ba, Ca, and Sr}$ ;  $\text{M} = \text{Co, Ni, and Mn}$ ;  $\text{B} = \text{Sb, Nb}$ ), *Chin. Phys. Lett.* **41**, 127502 (2024).
- [27] C. Zeng, D. J. J. Farnell, and R. F. Bishop, An efficient

implementation of high-order coupled-cluster techniques applied to quantum magnets, *J. Stat. Phys.* **90**, 327–361 (1998).

[28] D. Yamamoto, Correlated cluster mean-field theory for spin systems, *Phys. Rev. B* **79**, 144427 (2009).

[29] S. R. White and A. L. Chernyshev, Neel order in square and triangular lattice Heisenberg models, *Phys. Rev. Lett.* **99**, 127004 (2007).

[30] K. Harada, Numerical study of incommensurability of the spiral state on spin- $\frac{1}{2}$  spatially anisotropic triangular antiferromagnets using entanglement renormalization, *Phys. Rev. B* **86**, 184421 (2012).

[31] Z. Y. Xie, J. Chen, J. F. Yu, X. Kong, B. Normand, and T. Xiang, Tensor renormalization of quantum many-body systems using projected entangled simplex states, *Phys. Rev. X* **4**, 011025 (2014).

[32] Q. Li, H. Li, J. Zhao, H.-G. Luo, and Z. Y. Xie, Magnetization of the spin- $\frac{1}{2}$  Heisenberg antiferromagnet on the triangular lattice, *Phys. Rev. B* **105**, 184418 (2022).

[33] N. Read and D. Green, Paired states of fermions in two dimensions with breaking of parity and time-reversal symmetries and the fractional quantum hall effect, *Phys. Rev. B* **61**, 10267 (2000).

[34] T. D. Lee and C. N. Yang, Question of parity conservation in weak interactions, *Phys. Rev.* **104**, 254 (1956).

[35] D. Yamamoto and I. Danshita, Magnon supersolid and anomalous hysteresis in spin dimers on a triangular lattice, *Phys. Rev. B* **88**, 014419 (2013).

[36] T. Nishino and K. Okunishi, Corner transfer matrix renormalization group method, *J. Phys. Soc. Jpn.* **65**, 891 (1996).

[37] P. Corboz, J. Jordan, and G. Vidal, Simulation of fermionic lattice models in two dimensions with projected entangled-pair states: Next-nearest neighbor Hamiltonians, *Phys. Rev. B* **82**, 245119 (2010).

[38] R. Orús and G. Vidal, Simulation of two-dimensional quantum systems on an infinite lattice revisited: Corner transfer matrix for tensor contraction, *Phys. Rev. B* **80**, 094403 (2009).

[39] I. V. Lukin and A. G. Sotnikov, Variational optimization of tensor-network states with the honeycomb-lattice corner transfer matrix, *Phys. Rev. B* **107**, 054424 (2023).

[40] S. Nyckees, A. Rufino, F. Mila, and J. Colbois, Critical line of the triangular Ising antiferromagnet in a field from a  $C_3$ -symmetric corner transfer matrix algorithm, *Phys. Rev. E* **108**, 064132 (2023).

[41] Y. Zhang, Q. Yang, and P. Corboz, Accelerating two-dimensional tensor network contractions using QR-decompositions, [arXiv:2505.00494](https://arxiv.org/abs/2505.00494).

[42] H. Chen, Y. Fu, W. Yu, R. Yu, and Z. Y. Xie, A single-layer framework of variational tensor network states, [arXiv:2512.14414](https://arxiv.org/abs/2512.14414).

[43] A. I. Smirnov, H. Yashiro, S. Kimura, M. Hagiwara, Y. Narumi, K. Kindo, A. Kikkawa, K. Katsumata, A. Y. Shapiro, and L. N. Demianets, Triangular lattice antiferromagnet  $\text{RbFe}(\text{MoO}_4)_2$  in high magnetic fields, *Phys. Rev. B* **75**, 134412 (2007).

[44] Z. Tian, C. Zhu, Z. Ouyang, J. Wang, W. Tong, Y. Liu, Z. Xia, and S. Yuan, Susceptibility, high-field magnetization and esr studies in a spin-5/2 triangular-lattice antiferromagnet  $\text{Ba}_3\text{Mn}_{2.9}\text{Fe}_9$ , *Journal of Magnetism and Magnetic Materials* **360**, 10–14 (2014).

[45] D. Yamamoto, G. Marmorini, and I. Danshita, Microscopic model calculations for the magnetization process of layered triangular-lattice quantum antiferromagnets, *Phys. Rev. Lett.* **114**, 027201 (2015).

[46] D. Yamamoto, G. Marmorini, M. Tabata, K. Sakakura, and I. Danshita, Magnetism driven by the interplay of fluctuations and frustration in the easy-axis triangular XXZ model with transverse fields, *Phys. Rev. B* **100**, 140410 (2019).